Crystal Structures of Two H-2D[b]/Glycopeptide Complexes Suggest a Molecular Basis for CTL Cross-Reactivity

Ann Glithero,[1,8] Jose Tormo,[2,8]
John S. Haurum,[5] Gemma Arsequell,[6]
Gregorio Valencia,[6] Jon Edwards,[4]
Sebastian Springer,[4] Alain Townsend,[4] Ya-Lan Pao,[5]
Mark Wormald,[3] Raymond A. Dwek,[3] E. Yvonne Jones,[2]
and Tim Elliott[1,7]
[1] Nuffield Department of Clinical Medicine
University of Oxford
John Radcliffe Hospital
Oxford OX3 9DU
United Kingdom
[2] The Laboratory of Molecular Biophysics
[3] The Glycobiology Institute
Department of Biochemistry
University of Oxford
Oxford OX1 3QU
United Kingdom
[4] Institute of Molecular Medicine
John Radcliffe Hospital
Oxford OX3 9DU
United Kingdom
[5] The Danish Cancer Society
Institute of Cancer Biology
Copenhagen 2100
Denmark
[6] Unit for Glycoconjugate Chemistry
C. I. D. - C. S. I. C.
Barcelona E-08034
Spain

Summary

Two synthetic O-GlcNAc-bearing peptides that elicit H-2D[b]-restricted glycopeptide-specific cytotoxic T cells (CTL) have been shown to display nonreciprocal patterns of cross-reactivity. Here, we present the crystal structures of the H-2D[b] glycopeptide complexes to 2.85 Å resolution or better. In both cases, the glycan is solvent exposed and available for direct recognition by the T cell receptor (TCR). We have modeled the complex formed between the MHC-glycopeptide complexes and their respective TCRs, showing that a single saccharide residue can be accommodated in the standard TCR-MHC geometry. The models also reveal a possible molecular basis for the observed cross-reactivity patterns of the CTL clones, which appear to be influenced by the length of the CDR3 loop and the nature of the immunizing ligand.

Introduction

Major histocompatibility complex (MHC) class I and II molecules have evolved to present antigenic peptides at the cell surface, where they can be recognized by circulating T lymphocytes. In recent years, there has been increasing evidence to show that glycopeptides can also be presented by MHC molecules in the same way. Three examples of glycosylated antigens presented naturally by MHC class II have been reported to date, including an immunodominant epitope involved in the initiation of collagen-induced arthritis in mice (Michaelsson et al., 1994; Corthay et al., 1998) as well as the glycopeptide specificity of helper T cells recognizing bee venom phospholipase A2 in allergic human individuals (Dudler et al., 1995). There is also one report of a tumor-specific glycopeptide epitope presented by MHC class I (Zhao and Cheung, 1995). In all of these cases, glycopeptide-specific T cells have been isolated and have been found to depend on the glycan group for recognition. Several studies published in recent years have shown that synthetic glycopeptides carrying mono-, di- and tri-saccharides can both bind to MHC molecules and induce a T cell response. In at least some of these cases, the T cells induced are glycopeptide-specific and sensitive to the fine structure of the sugar (Haurum et al., 1994, 1995; Deck et al., 1995; Abdel-Motal et al., 1996; Jensen et al., 1997; Corthay et al., 1998), indicating that the sugar may be recognized directly.

In addition to the N- and O-linked glycosylation that occur in the endoplasmic reticulum (ER) and Golgi apparatus, O-β-linked N-acetylglucosamine (O-GlcNAc) substitution of serine and threonine residues is found abundantly on proteins in the cytosol and nucleus of mammalian cells (Hart et al., 1989). Since cytosolic protein is the preferred source of peptides for presentation by MHC class I molecules, it is possible that peptides carrying O-GlcNAc residues could enter the class I presentation pathway. We have shown that O-GlcNAc substituted peptides can be efficiently translocated across the ER membrane by the transporter associated with antigen processing (TAP) (Haurum, 1996) and that synthetic glycopeptides carrying single O-GlcNAc residues can bind to the murine class I molecule H-2D[b] and are immunogenic (Haurum et al., 1994, 1995), giving rise to glycan-specific CTL. Two O-GlcNAc substituted peptides were used, both being analogs of the Sendai virus nucleoprotein residues 324–332 (FAPGNYPAL). This peptide binds to H-2D[b] using the side-chains asparagine at position 5 and leucine at position 9 as anchor residues (Haurum et al., 1994). The glycopeptide analogs, FAPS(O-GlcNAc)NYPAL (designated K3G) and FAPGS(O-GlcNAc)YPAL (designated K2G) thus carry the substitutions on positions 4 and 5, respectively. In the case of K2G, this is a modification of the P5 anchor residue.

We have raised H-2D[b] CTL against both of these glycopeptides in C57Bl/6 mice. Surprisingly, immunization with K2G readily elicited an H-2D[b]-restricted CTL response despite the fact that it binds 100-fold less strongly to H-2D[b] than the unsubstituted or wild-type peptide (Haurum et al., 1995). Several K3G- and K2G-specific CTL clones were isolated and shown to require the glycan for recognition. We found that all the H-2D[b]-restricted K2G-specific clones exhibited a strong cross-reactivity toward K3G. In fact, in peptide titration experiments, the K2G-specific clones tended to recognize

[7] To whom correspondence should be addressed (e-mail: tim.elliott@ndm.ox.ac.uk).
[8] Both authors contributed equally to this work.

WT	FAPGNYPAL
K3G	FAPS(O-β-GlcNAc)NYPAL
K2G	FAPGS(O-β-GlcNAc)YPAL

Figure 1. Peptide Structures

The peptides used in this study are based on an H-2D^b restricted CTL epitope (WT) from Sendai Virus nucleoprotein residues 324–332. K3G and K2G carry the Ser-*O*-GlcNAc substitution at positions 4 and 5 on the peptide backbone, respectively. The anchor residues for peptide binding to H-2D^b are underlined.

K3G at concentrations three orders of magnitude lower than the concentration of K2G required to elicit the same response. In addition, K3G-specific clones recognized K2G very poorly or not at all. Despite these differences in cross-reactivity, the T cell receptors (TCR) selected by K2G- and K3G-specific CTL were remarkably similar and in one case, the highly cross-reactive anti-K2G TCR differed from a highly specfic anti-K3G TCR by only five amino acids, including a two amino acid reduction in length, in the junctional region of the β chain (Haurum et al., 1995).

In order to investigate the recognition of MHC class I-glycopeptide complexes by CD8^+ cytotoxic T lymphocytes (CTL) in more detail, we have determined the X-ray crystal structures of the WT peptide and the two N-acetylglucosamine-bearing glycopeptides complexed with the murine class I allele H-2D^b. Using existing MHC class I/TCR crystal structures as a basis, we have also modeled the glycopeptide-specific TCR clones raised against both K2G and K3G onto our MHC-glycopeptide complexes. Here, we relate the striking differences in the specificity of the clones to the structures of their TCRs and the immunizing ligands and suggest a molecular basis for CTL cross-reactivity to glycopeptide antigens.

Results and Discussion

The peptides used in this investigation (Figure 1) are synthetic glycopeptide analogs of the immunodominant CTL epitope FAPGNYPAL from Sendai virus nucleoprotein residues 324–332 (Rotzschke et al., 1991). The glycopeptide analogs K3G and K2G carry the *O*-GlcNAc residue attached to a serine substitution at P4 and P5, respectively. Recombinant, soluble H-2D^b class I molecule (comprising heavy chain residues 1–284 followed by six histidine residues bound to humanβ_2m [Springer et al., 1998]), was crystallized in complex with the wild-type (WT) peptide, K3G, K2G, and the unglycosylated peptide FAPGSYPAL (K2), allowing the corresponding series of three-dimensional structures to be determined by molecular replacement and refined at a resolution of 2.85 Å or better (see Experimental Procedures). The overall structures of the different H-2D^b-peptide complexes reported in this work are very similar to those of other MHC class I molecules, both mouse and human (Madden, 1998). For example, the superposition of the α1/α2 domains onto those of H-2D^b complexed with an Influenza virus peptide (Young et al., 1994) gives an
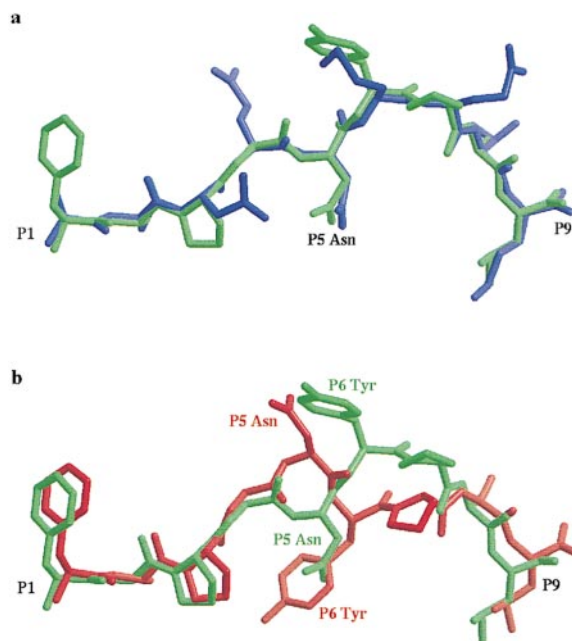

Figure 2. Crystal Structure of the WT Peptide FAPGNYPAL Complexed with H2D^b

(A) The structure of WT (green) is shown superposed with the previously reported structure of the peptide ASNENMETM (blue) complexed with H-2D^b. (B) The structure of WT when complexed with H2-D^b (green) is shown superposed with the previously reported structure of WT when complexed with H-2K^b (Fremont et al., 1992) (red). Components of this figure and Figures 3, 4, 5, and 7 were drawn using programs BOBSCRIPT (Esnouf, 1997) and Raster3D (Merritt and Murphy, 1994) and structural superpositions were performed using the program SHP (Stuart et al., 1979).

average root-mean-square (r.m.s) difference in Cα positions of 0.56 Å. The greatest difference between these complexes and those of other MHC class I molecules is found in their quaternary structure, especially in the pairing between the β2m and α3 domains, which will be described elsewhere. In the following sections, the analysis of the structures will therefore be confined to the peptide-binding groove.

Crystal Structure of the Wild-Type H-2D^b/FAPGNYPAL Complex

Figure 2A compares the conformation of the current FAPGNYPAL peptide with that of the only other H-2D^b peptide complex reported to date (between H-2D^b and the influenza virus nucleoprotein peptide ASNENMETM [Young et al., 1994]). The side-chains of peptide residues P2, P3, P5, and P9 are buried in the binding groove in both complexes, and the main-chain conformation of the two peptides is essentially identical (r.m.s. deviation for the nine Cα positions is 0.35 Å). This degree of conserved conformation between bound peptides is markedly greater than that generally observed within sets of nonamer peptides bound to common MHC class I molecules (Fremont et al., 1992; Garboczi et al., 1994; Smith et al., 1996). The dominant role of asparagine at P5 in the H-2D^b anchor motif and the steric restrictions placed on P6 and P7 side-chain orientation by a distinctive hydrophobic ridge within the H-2D^b binding groove

(Young et al., 1994) may place unusually tight limits on the conformation of nonamer peptides with the H-2D^b binding motif when bound in the groove.

The Sendai virus nucleoprotein-derived peptide FAP-GNYPAL is an immunodominant H-2K^b-restricted CTL epitope (Kast et al., 1991), as well as having the appropriate anchor residues for binding to H-2D^b. The peptide conformation in the current H-2D^b/FAPGNYPAL complex and in the previously reported H-2K^b/FAPGNYPAL complex (Fremont et al., 1992) is, however, very different for residues P4-P7 as a result of the different shapes of the peptide binding groove of these two MHC class 1 alleles and their different anchor motif specificities (r.m.s. on equivalent Cα positions is 1.9 Å, Figure 2B). This provides a particularly clear demonstration of the influence of the MHC class I binding groove in determining the conformation of the bound peptide.

As expected from the H-2D^b anchor motif and previous peptide-binding and X-ray crystallographic studies (Haurum et al., 1994; Young et al., 1994), the H-2D^b/FAPGNYPAL structure shows that the glycopeptide analogs K3G and K2G represent substitutions at peptide residue side-chains that are respectively solvent exposed and buried in the WT complex.

Crystal Structure of H-2D^b Complexed with K3G

The crystal structure of the H-2D^b/FAPS(O-GlcNAc)NYPAL (K3G) complex, in which the O-GlcNAc is attached to peptide position P4, shows clearly that the sugar residue is solvent exposed and projects above the level of the α1 and α2 helices (Figures 3A and 3B). There is no significant change in the conformation of the K3G peptide backbone within the H-2D^b binding groove compared to that of the WT peptide (r.m.s. on equivalent Cα positions is 0.35 Å). In addition, the orientation of the peptide side-chains is unaltered except at the P6 tyrosine, which reorientates slightly in order to stack against the GlcNAc pyranose ring (Figure 3C). The reported glycan specificity of CTL generated to this structure (Haurum et al., 1995) is therefore likely to be due to direct recognition of the sugar and not due to the recognition of a glycosylation-induced conformational change in the bound peptide, as has been suggested previously for some class II MHC restricted glycopeptide-specific T cells (Harding et al., 1993). Indeed, over 48% of the exposed peptide surface area is accounted for by the glycan, which could therefore make a major contribution to the contact surface between the T cell receptor and the MHC:glycopeptide complex.

The X-ray crystallographic analysis bias free electron density (calculated in the absence of any model for the sugar) indicates the occurrence of two major conformations for the O-GlcNAc residue, each at similar occupancy. Only one of these conformations is shown here (see Figure 3); the second is rotated approximately 180° around the O-glycosidic bond. The sugar ring is orientated in a similar plane for both conformations and there is some packing against the aromatic side-chain of the tyrosine at peptide residue P6, which in turn stacks against histidine 155 on the MHC α2 helix (Figure 3D). Indeed, the electron density of the P6 side-chain is somewhat distorted in a manner consistent with some

coupling of O-GlcNAc and tyrosine side-chain conformations. Stacking of the GlcNAc pyranose against aromatic residues is a common feature of the carbohydrate binding sites of both lysozyme and wheatgerm agglutinin (Quiocho, 1998). Here, this interaction appears to limit the O-GlcNAc conformation to an equilibrium between two orientations. In both conformations, the glycan is solvent exposed and available for direct recognition by TCRs of glycopeptide-specific CTL, particularly via the hydoxyl groups of the hexose ring.

Crystal Structure of H-2D^b Complexed with K2G

In contrast to the structure with K3G, the complex with the second glycopeptide, K2G, differs profoundly from the WT and K3G structures (r.m.s. deviation of 1.4 Å, Figure 4). The bulky O-GlcNAc ring is too large to be accommodated in the peptide binding groove in the same way as the asparagine anchor residue usually found at this position, and as a result the peptide backbone has been forced to undergo a major local rearrangement, involving rotation of the peptide backbone encompassing residues P4-P7 by 180°, compared with WT (Figure 4C). This results in the orientation of the glycan on K2G away from the peptide binding groove rendering it exposed to solvent. In addition, the central portion of the peptide is positioned further above the binding groove with the Cα positions of residues P4 and P5, respectively, some 0.7 and 3.6 Å higher than in WT. The peptide backbone of K2G is more mobile than K3G, and this mobility is particularly evident around P4 to P6 as deduced from crystallographic B factors (see Experimental Procedures).

Of the peptide side-chains common to the exposed surfaces of the WT, K3G, and K2G complexes, the conformation of the tyrosine side-chain at P6 is very different in K2G (see also Figure 4C). The aromatic ring of the P6 tyrosine reorientates downward to stack parallel with that of MHC residue Tyr$_{156}$ at the side of the peptide binding groove. This rearrangement allows the sugar to project out of the binding groove. The sugar in the K2G complex makes no favorable interactions with H-2D^b comparable to the ring-stacking interaction present in K3G; however, it again adopts a small number of different conformations. Electron density (calculated in the absence of any sugar coordinates) delineates a crown-shaped arc indicative of at least three major sugar conformations (Figures 4A and 4B).

An asparagine at P5 is a clear feature of the H-2D^b peptide binding motif and corresponds to the formation of hydrogen bonds between the polar groups of the P5 asparagine side-chain and those of the MHC residue glutamine 97 (Gln$_{97}$) side-chain. For K2G, in the absence of a P5 asparagine anchor, alternative polar groups are required to satisfy the hydrogen bonding potential of Gln$_{97}$. One possible source of such groups is the sugar (Haurum et al., 1995); however, the current analysis clearly demonstrates that in this case, two water molecules fulfil this role (Figure 4D). As a result, the structure of the H-2D^b binding groove in the K2G complex is essentially unperturbed from that of the WT complex. The crystal structure for the H-2D^b/FAPGSYPAL (K2) complex (data not shown) indicates that a P5 serine residue
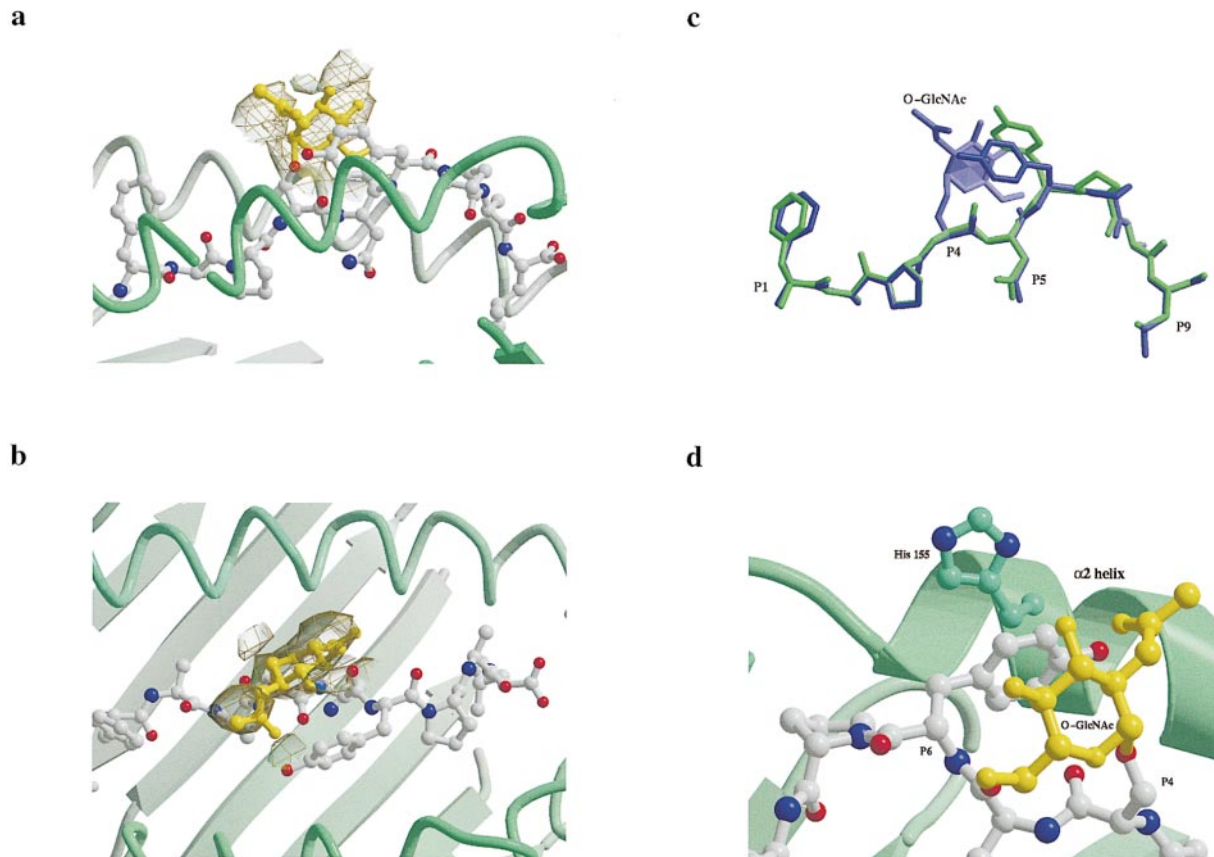
Figure 3. Crystal Stucture of H-2D^b Complexed with the Glycopeptide K3G

(A) The mainchain of H-2D^b is shown schematically in pale green and the peptide is depicted in ball-and-stick representation with the glycan highlighted in yellow. Bias free 2FO-Fc electron density (calculated after rigid body refinement prior to the inclusion of any model for the glycan, see Experimental Procedures) is shown as shaded chicken wire. The view is into the side of the peptide-binding groove through the α2 helix.

(B) Same as in (A) but viewed down onto the binding groove.

(C) The structure of the K3G peptide when complexed with H-2D^b (blue) is shown superposed with the WT structure (green). In the WT complex, histidine 155 stacks against tyrosine 156 and donates a hydrogen bond to the carbonyl of glycine at P4, as in the H-2D^b-Influenza virus complex (Young et al., 1994), while tyrosine at P6 stacks against histidine 155. In K3G, tyrosine at P6 is oriented with its side-chain aromatic ring perpendicular to that of tyrosine 156, while the histidine 155 side chain has flipped pointing away from the binding groove, parallel to tyrosine at P6. The hydrogen bond between the histidine 155 side chain and the peptide is lost. Tyrosine at P6 has probably reoriented in order to stack against the GlcNAc ring.

(D) The stacking of the K3G glycan, P6 tyrosine, and histidine 155 rings. The view is through the α1 helix (i.e., rotated through the O-glycosidic bond by some 180° relative to that of 3A).

can also mediate one of the standard hydrogen bonds such that the unglycosylated form of the peptide (FAPG-SYPAL) binds H-2D^b with essentially the same conformation as the optimal, tight-binding peptide of the WT complex (data not shown) albeit with much lower affinity (Haurum et al., 1995).

Mobility of the Attached Glycan

The X-ray crystallographic analyses of the K3G and K2G complexes established that the attached O-GlcNAc is solvent exposed in both glycopeptide complexes and occupies an overlapping region of space, despite being positioned on two neighboring residues in the peptide (Figures 3 and 4). In both complexes, the glycan enjoys some degree of conformational freedom, with electron density indicative of a small set of distinct conformations. Although this conformational variability is limited,

it is more extensive than that seen for amino acid side-chains of MHC-bound peptides in previously described crystal structures.

We have used proton nuclear magnetic resonance relaxation rate studies (CPMG) to investigate the mobilities of carbohydrates in relation to the protein to which they are attached (Wormald et al., 1997). CPMG experiments on both K2G and K3G complexes indicated that the saccharide residues have similar dynamic properties to the majority of the protein amino acid side-chains, since peaks corresponding to the glycans were not detected in the CPMG experiments (data not shown). This technique is sensitive to oscillations over 3 Å that occur significantly faster than the rate of protein tumbling in solution—in practice on a timescale of 10^{-6} to 10^{-8} sec. Since the electron densities for K2G and K3G show a range of conformations that are separated by greater than 3 Å, it is reasonable to conclude that the attached
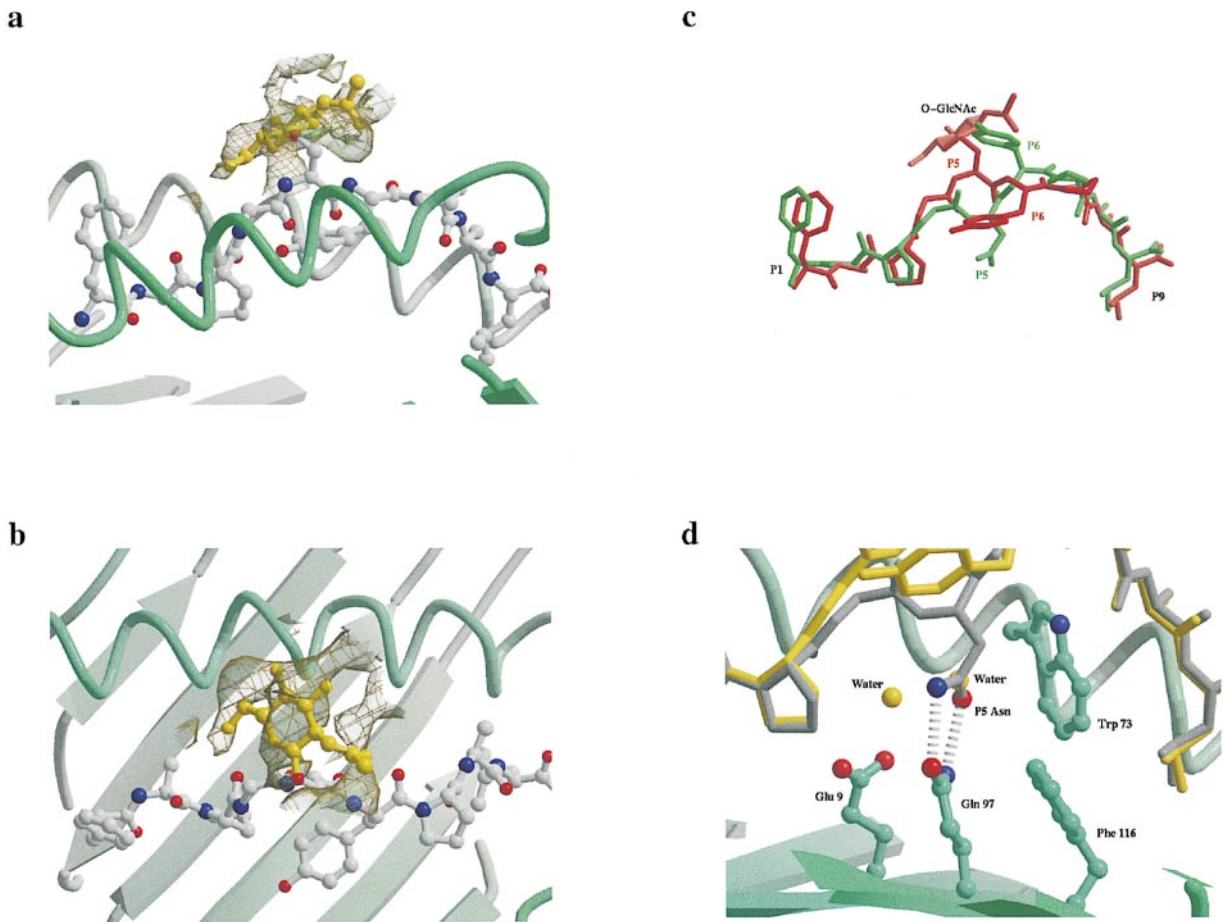
Figure 4. Crystal Stucture of H-2D^b Complexed with the Glycopeptide K2G

(A) The mainchain of H-2D^b is shown schematically in pale green, the peptide is depicted in ball-and-stick representation with the glycan highlighted in yellow. Bias free 2FO-Fc electron density (calculated after rigid body refinement prior to the inclusion of any model for the glycan, see Experimental Procedures) is shown as shaded chicken wire. The view is into the side of the peptide-binding groove through the α2 helix.

(B) As for (A) but viewed down onto the binding groove.

(C) The structure of the K2G peptide when complexed with H-2D^b (red) is shown superposed with the WT structure (green).

(D) The C pocket. The mainchain of H-2D^b, which is essentially unchanged in conformation between the WT and K2G complexes, is depicted schematically in pale green with selected MHC residue side-chain positions (also essentially unchanged between complexes). The WT peptide structure with P5 Asn anchor residue is shown as a stick representation in gray. The K2G complex structure is shown superposed as a stick representation in yellow. Hydrogen bonds in the WT complex are depicted as broken lines. The view is into the side of the peptide-binding groove through the α2 helix.

sugars do not oscillate between their various conformations on this timescale.

TCR Recognition: Implications of the K3G and K2G Structures for T Cell Cross-Reactivity

We have previously shown that a number of CTL clones generated to the glycopeptides K2G and K3G select surprisingly similar TCR sequences (Haurum et al., 1995). For example, CTL clones K2G.6.9 and K3G.5.8, raised against the K2G and K3G complexes, respectively, express TCRα chains that are identical at the amino acid level (although they differ by one nucleotide in the junctional region). They also share a common TCR Vβ and Jβ segment usage. They therefore differ only in the junctional region encoding the third complementarity-determining region (CDR3) loop of the β chain for which K2G.6.9 has the sequence LGANERLF and K3G.5.8 has the sequence FPGQSNERLF. All these TCR

clones are glycopeptide-specific, i.e., they do not recognize the unglycosylated peptides K3 (FAPSNYPAL), K2 (FAPGSYPAL), or the WT peptide. Despite the similarity between the TCR sequences, the clones have markedly different patterns of cross-reactivity. K2G.6.9, although raised against H-2D^b/K2G, is highly cross-reactive, efficiently killing targets pulsed with K3G. In contrast, K3G.5.8, raised against H-2D^b/K3G, is highly specific, recognizing only that peptide (Haurum et al., 1995). These data can now be usefully reassessed in the context of the H-2D^b/K2G and H-2D^b/K3G crystal structures. The crystal structure for an MHC class I/TCR complex (Garboczi et al., 1996) provided the basis for a simple modeling exercise to relate the TCR sequence data to the characteristics of the TCR recognition surfaces presented by the K2G and K3G complexes.

The preliminary, low resolution complex of a murine TCR with H-2K^b (Garcia et al., 1996) and the refined HLA

A2/TCR complex of Garboczi and coworkers (Garboczi et al., 1996) revealed a common orientation of the TCR relative to the MHC class I/peptide complex. Subsequent, refined, crystal structures for MHC class I/TCR complexes (Ding et al., 1998; Garcia et al., 1998) have further reinforced the concept of a basic standard geometry for the interaction and in particular highlight the conservation of the TCR α chain docking geometry. For the K2G and K3G complexes, this implies that the CDR 3 loops of the TCR α and β chains will be positioned over the central portion of the peptide as shown in Figure 5. Several important points are immediately apparent from this juxtaposition of MHC class I complex and TCR. The model shows that the glycan of both K3G (Figures 5A–5C) and K2G (Figures 5D–5F) is accommodated in a central cavity formed between the two CDR3 loops at the interface between the TCR α and β chains. Secondly, the size of this cavity may impose some restrictions on the number of conformations that the glycan could adopt when it is part of a complex with the glycan-specific TCR. For the K3G complex sugar, one conformation can certainly be accommodated within the standard complex interface as shown in Figure 5A, but the second (data not shown) may be disfavored since this sugar position would occlude the standard TCR α chain positioning by interfering with the αCDR2.

Similarly, not all of the arc-shaped space encompassing the different sugar conformations in the K2G complex can be accommodated by a standard TCR interface. However, the shorter βCDR3 loop of the K2G-specific TCR, which contains small amino acid side-chains at positions 101 and 102 (Gly and Ala compared to Gln and Ser in the βCDR3 of the K3G-specific TCR) is likely to generate a larger pocket between the αCDR3 and βCDR3 loops. This selection of a shorter βCDR3 loop may be essential to mitigate enthalpic penalties if the TCR is to accommodate one or more of the arc of conformations adopted by the glycan in K2G. Indeed, it is possible that since the glycan of K2G may oscillate between conformations on a timescale comparable to the lifetime of the TCR:MHC complex (i.e., longer than 10^{-6} sec), a shorter CDR3 loop may be selected by K2G in order to allow the glycan to remain mobile when the TCR is bound. This would also have the effect of reducing the entropic penalty upon TCR binding. This latter possibility is notable in light of recent evidence from a kinetic and thermodynamic analysis that the affinity of T cell receptor binding to its class I MHC:peptide ligand is dominated by unfavorable entropic effects (Willcox et al., unpublished data). It is important to note, however, that a significant amount of tilt, rotation, and translocation is seen on comparison of the binding orientation of TCRs in different MHC class I/TCR complexes (Ding et al., 1998; Garcia et al., 1998; Teng et al., 1998), indicating that there is some variability of docking orientations within the standard TCR positioning that may not be represented by the models shown in Figure 5.

These models suggest a molecular basis for the cross-reactivity of CTL clones raised to K2G. In these models, the glycans of both K2G and K3G are accommodated in a similar manner by their respective TCR—that is, in a central glycan binding pocket formed between the CDR3 loops. Many of the major interactions of the TCR

α subunit and the βCDR1 and 2 loops, common to both clones, are with the regions of the MHC recognition surface that are essentially identical between K2G and K3G. Although it is difficult to assess the direct interaction of TCR and glycan from the simple modeling, the glycan interactions may be similar for the two receptors. Possible TCR contact residues on the α chain, which are shared by both CTL clones (tyrosine 31, Y_{31}, and tyrosine 100, Y_{100}), are shown in Figures 5B, 5C, 5E, and 5F. The potential TCR contact residues on the βCDR3 loop are also shown. Although the sequence of this loop differs between the two clones, they have both selected asparagine at position 103 (N103) and glutamate at position 104 (E104). These have polar side-chains suitable for hydrogen bonding with the sugar hydroxyls. It is therefore likely that a common glycan binding pocket with similar TCR-sugar contacts allows the CTL raised to K2G to cross-react with K3G.

In contrast, the clone raised against K3G (K3G5.8) does not reciprocally recognize K2G. As well as the increased volume of space occupied by the K2G glycan compared to that of K3G, the P4-P5 portion of K2G is more prominent, lying some 3.6 Å further above the binding groove than for K3G, raising the position of the glycan slightly relative to the α1 and α2 helices of H-2D^b (see Figure 4). In addition, the glycan group in K2G lies further toward the C terminus of the peptide and is orientated such that it extends off the medial line of the peptide-binding groove and substantially closer to the α1 helix of the H-2D^b molecule. The lateral positioning and greater number of conformations of the K2G glycan, along with the increased mobility of the peptide backbone supporting it, may make it less easily accommodated between the αCDR3 and βCDR3 loops of K3G5.8 than the K3G glycan. As discussed earlier, this is likely to impact on the ability of the TCR β chain to contribute fully to the interface with K2G. This simple observation accords well with the observed difference in the length of the βCDR3 loop: the only difference between the TCR of CTL clones raised against K2G and K3G. The failure of K3G.5.8 to cross-react with K2G is most likely to be a direct result of its longer βCDR3 loop, which would be less likely to accommodate the prominent P4-P5 and glycan of this peptide. A similar situation has been described recently (Ding et al., 1998) for two TCR surfaces that contact the same MHC/peptide complex in which differences in reactivity could be attributed to the different-sized pockets between the TCR α and β subunits that in that system accommodate the peptide ligand P5 side-chain.

TCR Recognition: Implications of the K3G and K2G Structures for T Cell Promiscuity

In order to investigate the contribution of interactions between the peptide amino acid side-chains and TCRs expressed by both specific and cross-reactive CTL, we tested the ability of H-2D^b-restricted CTL clones K3G.6.15 and K2G.6.9 to recognize K3G analogs carrying alanine substitutions in the C-terminal half of the peptide that would be expected to make contact with the βCDR3 loop. As was the case for clone K3G5.8 (see above), clone K3G.6.15 does not cross-react with K2G
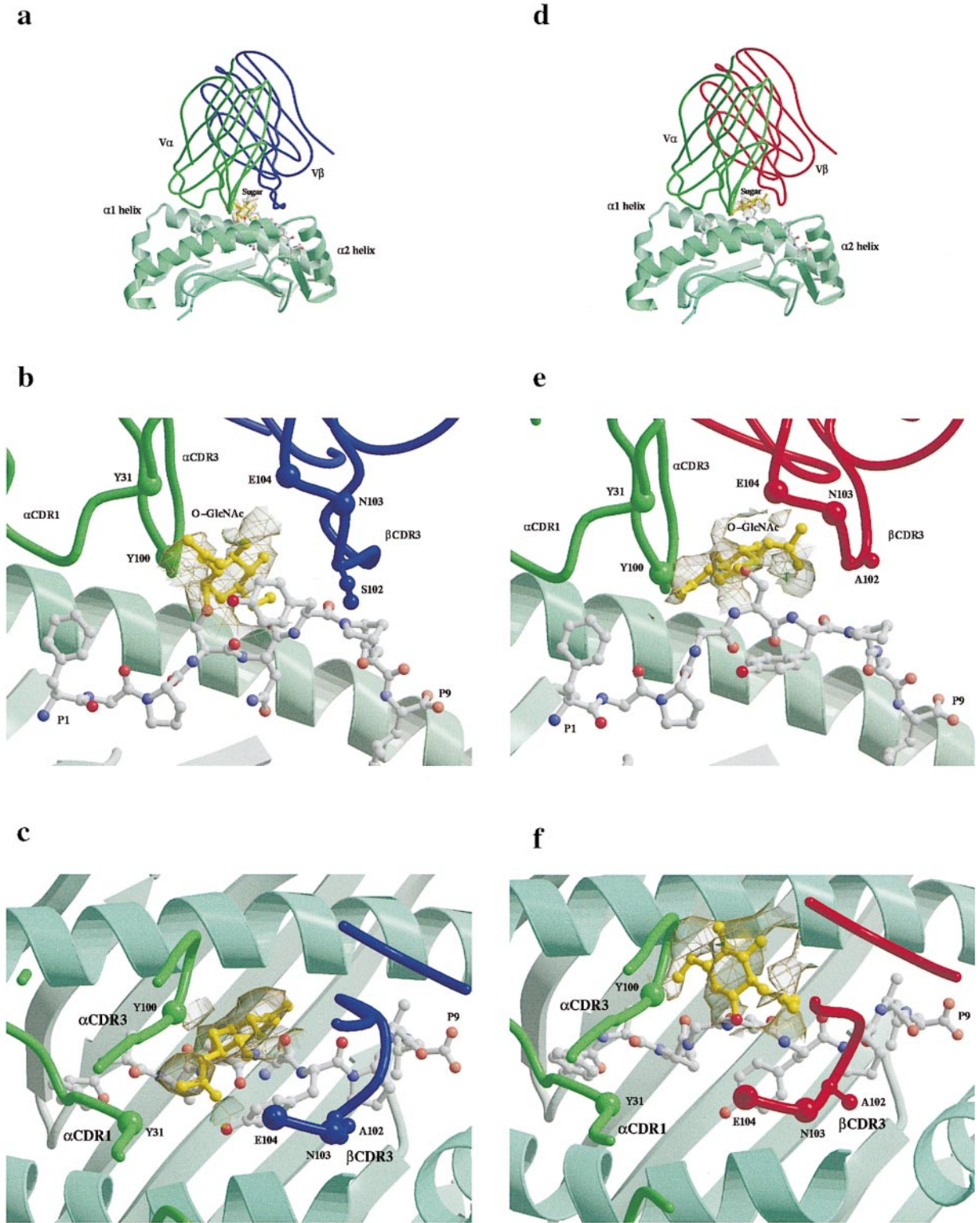
Figure 5. Molecular Models Showing the K3G and K2G Structures in the Context of the Standard Docking of MHC Class I and TCR

(A) A model for the TCR of glycopeptide-specific CTL clone K3G.5.8 is shown positioned over the K3G structure (by comparison with published TCR-MHC co-crystal complexes, see Experimental Procedures). The main-chain is shown schematically for the TCR α chain (green), TCR β chain (blue) and H-2D^b (pale green). The peptide is depicted in ball-and-stick representation with the glycan highlighted in yellow. The electron density of Figure 3 is also overlaid onto the figure to emphasize the full range of sugar conformations observed experimentally in the unliganded MHC class I crystal structure. The view is into the side of the peptide-binding groove through the α2 helix and is shown in close up in (B) with the α2 helix of H-2D^b removed for clarity. (C) Same as in (B) but viewed down onto the binding groove. (D–F) A model for the TCR of glycopeptide-specific CTL clone K2G.6.9 is shown positioned over the K2G structure. The view in (D), (E), and (F) is as in (A), (B), and (C), respectively.
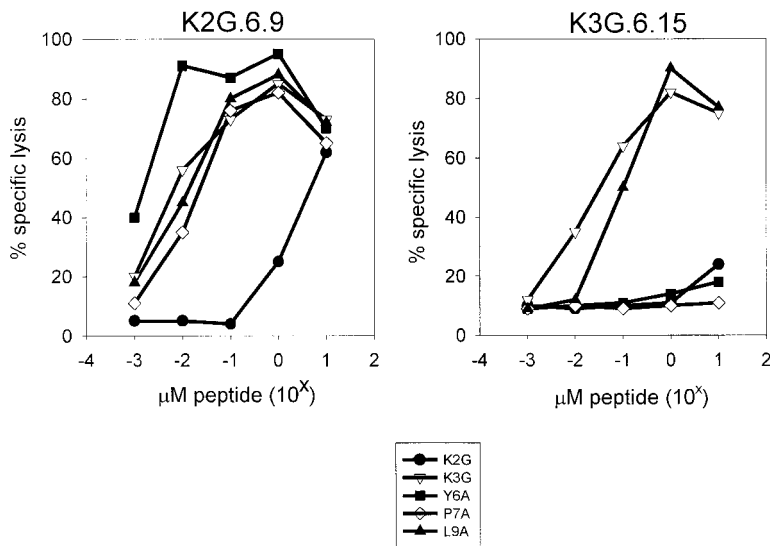
K2G.6.9 K3G.6.15

Figure 6. Anti-K2G CTL Are More Promiscuous than Anti-K3G CTL

Peptide specificity of CTL clones K2G.6.9 (raised against K2G) and K3G.6.15 (raised against K3G) tested against ^{51}Cr-labeled target cells T2-D^b in the presence of K3G (upside down triangle), K2G (closed circle), K3G with a tyrosine to alanine substitution at position 6 (closed square), K3G with a proline to alanine substitution at position 7 (open diamond), and K3G with a lysine to alanine substitution at position 9 (closed triangle).

(Figure 6) and is therefore representative of the K3G-specific CTL clones, while K2G.6.9 is reactive to both K2G and K3G complexes (Figure 6).

Figure 6 also shows that K2G.6.9, but not K3G.6.15, could tolerate alanine substitutions at peptide positions 6 and 7. Thus, the two CTL clones differ markedly in their sensitivity to the variant peptide ligands bearing changes at the exposed P6 and P7 side-chains but not at the buried P9 anchor. Once again, K2G.6.9 displays a broader spectrum of reactivity than CTL clones raised against K3G.

The CTL clones K2G.6.9 and K3G.6.15 express the same TCR Vβ segment that encodes the βCDR1 and 2 loops but differ in the junctional region corresponding to the βCDR3 loop (the sequence for K3G.6.15 is LELSQNTLY [Haurum et al., 1995]). The βCDR3 loop of clone K3G.6.15 was modeled in the same way as described above, using the crystal structure of the HLA A2/TCR complex (Garboczi et al., 1996) as a template. Figure 7 shows that, as above, the CDR3 loop of K3G.6.15 (blue), like that of K3G.5.8, is extended relative to that in K2G.6.9 (red), by virtue of being one residue longer and having a serine at position 102 rather than alanine and leucine at position 101 rather than glycine. K3G.6.15 may therefore have considerable contact with the peptide at P6 and P7, mediated perhaps by hydrogen bonding through serine 102 and/or van der Waals contacts through leucine 101 of the TCR. The shorter loop of K2G.6.9 would be less likely to make this contact. This local difference in TCR structure is fully consistent with the difference in the ability of the CTL to tolerate alanine substitutions at P6 and P7 in the recognition surface presented by the K3G complex. Interestingly, both K3G.6.15 and K2G.6.9 were sensitive to an alanine substitution at P1 (data not shown) that is solvent exposed and would be expected to make contacts with the TCRα chain.

There are therefore two consequences of selecting a short βCDR3 loop in response to antigenic challenge by K2G presented by H-2D^b. The first is that it allows access of the K2G glycan—which occupies a large volume of space—to a central binding pocket, which is

formed by residues of both the TCR α and β chain. The second is that it disfavors contact between the CDR3 loop of the TCR β chain and the peptide part of the glycopeptide ligand. The shorter βCDR3 loop may also have been selected to allow the region of the bound K2G peptide around P6 and P7 (which lie directly below this loop in our models), as well as the glycan, to remain mobile, thus minimizing the loss of entropy upon TCR binding. Taken together, these lead to the selection of a highly promiscuous TCR that displays a high degree
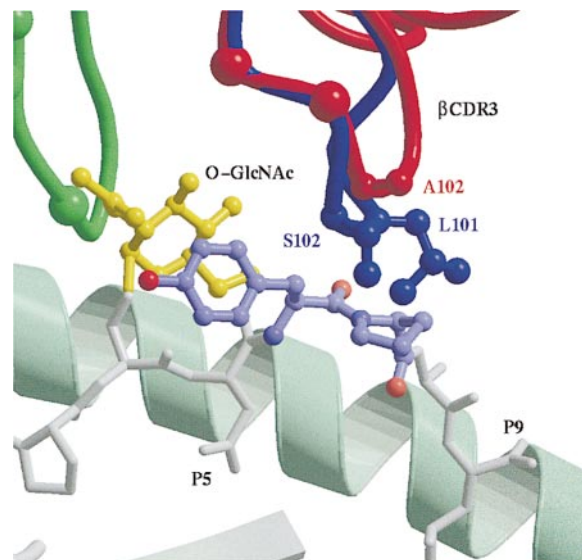

Figure 7. Molecular Models of K3G- and K2G-Specific TCR Recognizing the H-2D^b/K3G Complex

The TCR models were positioned by comparison with published TCR-MHC co-crystal complexes (see Experimental Procedures). The mainchain is depicted schematically for the K2G.6.9 α chain (green), K2G.6.9 β chain (red), and K3G.6.15 β chain (blue). Potential TCR-sugar contact residues are marked as spheres at C α positions. With the exception of the TCR β position 101 and 102 amino acid, side-chains have been omitted. Residues at peptide positions P6 and P7 are highlighted in pale blue. The view is into the side of the peptide-binding groove through the α 2 helix.

of cross-reactivity toward variant peptides, e.g., K3G (in which the glycan occupies a smaller but overlapping volume of space) and K3G alanine substitutes.

Perspectives

The recognition of O-GlcNAc modified peptides by T cells could be highly significant as glycosylation could create a T cell neoepitope without requiring a change at the genetic level. Alterations in intracellular metabolism that lead to changes in posttranslational modifications including cytosolic glycosylation are known to occur in development, autoimmunity, and malignancy. O-GlcNAc is known to be dynamically regulated and levels change in response to cellular activation (Hart et al., 1996). Also, many pathogen antigens including viral, trypanosomal, schistosomal, leishmanial, and malarial proteins are O-GlcNAc modified (Hart et al., 1989).

We have shown that the O-GlcNAc group of two H-2D^b-associated glycopeptides is solvent exposed and therefore available for direct recognition by TCR, supporting the conclusion that glycopeptide-specific CTL recognize the glycan directly. This idea is further supported by our models of glycopeptide-specific TCR that appear to have conserved amino acid side-chains that are of an appropriate location and chemical nature to interact with serine modified with O-GlcNAc. These models also indicate that the sugar ring is small enough to allow TCR to contact peptide and MHC simultaneously.

In the case of K2G, where the substitution is on a peptide-anchor position, the sugar profoundly affects the conformation of the bound peptide in the H2-D^b groove. Thus, the region of the peptide immediately surrounding the Ser-O-GlcNAc is rotated through 180° in such a way as to expose the glycan to solvent. This leaves a specificity-determining pocket in the H2-D^b peptide-binding groove empty and H-bonds that are normally formed with the N anchor side-chain are instead made with water molecules.

The O-GlcNAc of K3G adopts two conformations, which together occupy a relatively restricted volume of space of around 260 Å^3, whereas the same sugar in K2G adopts at least three conformations that may occupy a volume of space of up to double that in K3G. It is unlikely that the glycan exchanges between these conformations rapidly (1×10^{-6} to 1×10^{-8} sec) but may nevertheless still exchange on a timescale that is comparable with the lifetime of the TCR:MHC complex. This degree of conformational variation has so far not been seen for amino acid side-chains of peptides bound to MHC class I molecules, and whether it is a general property of carbohydrate-modified side-chains remains to be seen. For these structures, the flexibility of the glycan side-chains seem to contribute to the pattern of cross-reactivity we have observed between CTL raised to the two glycopeptides.

We have exploited the small differences in the sequence of three glycopeptide-specific TCRs with strikingly different patterns of recognition in order to interpret T cell cross-reactivity at the molecular level. In summary, the highly cross-reactive CTL clone K2G.6.9 recognized both glycopeptides by virtue of (1) the necessarily large cavity required to accommodate the K2G glycan also encompassing the space occupied by one of the K3G sugar conformations and (2) some common TCR-sugar contacts. Some of these contacts, for example with histidine 29 and asparagine 30 of the βCDR1, could explain the striking preference for Vβ11 segment-usage by CTL raised to O-GlcNAc modified peptides; and tyrosine 31 on the αCDR1 for the preferential use of Vα5.3.18 (Haurum et al., 1995). Interestingly, several motifs that were found among the βCDR3 loops of O-GlcNAc-specific CTL ("NERLF", "SYEQ," and "SAETLY" [Haurum et al., 1995]) have also recently been observed among MHC class II restricted T cells recognizing glycopeptides with hydroxylysine-linked Galactose modifications (Corthay et al., 1998). The specificity of CTL clones K3G.5.8 and K3G.6.15 seems to be determined in part by their longer βCDR3 loop that may limit the size of the "glycan binding pocket" in such a way as to restrict the access of O-GlcNAc of K2G, which occupies several conformations within a larger volume of space and in a slightly different position. The long βCDR3 loop of K3G.6.15 also results in greater selectivity at p6 and p7, which probably make contacts with this loop.

A high degree of cross-reactivity may be an intrinsic and necessary feature of T cell reactivity (Mason, 1998). It is the underlying feature of several important immunological phenomena such as positive selection in the thymus (Bevan, 1997), alloreactivity (Brock et al., 1996), and autoimmunity (Sinha et al., 1990), and yet the molecular basis for such cross-reactivity has so far remained relatively unexplored. Molecular mimicry is thought to be an important mechanism in experimental autoimmune diseases such as adjuvant arthritis in rats (van Eden et al., 1988), Arthritides (Fielder et al., 1995), and in inflamatory CNS disease (Wucherpfenning and Strominger, 1995; Steinman, 1996). Our results provide a picture of how molecular mimicry by two related ligands can be interpreted at the T cell level. This particular model is interesting because it illustrates two ways in which a highly cross-reactive (i.e., potentially autoreactive) CTL could be generated. The first conforms to the classic model of molecular mimicry in which a viral glycopeptide (e.g., K2G) elicits a highly cross-reactive T cell response that encompasses recognition of a self-peptide (e.g., K3G or any of the alanine substitutions). In the second, a neoepitope could be generated following the aberrant glycosylation of a self peptide (e.g., glycosylation of K2 to give K2G), leading to an anti-self (e.g., anti-K3G) reactivity.

Experimental Procedures

Peptide Synthesis
Peptides and glycopeptides were synthesized as described in Haurum et al. (1994).

Protein Expression, Purification, and Crystallization
Purified, peptide receptive H-2D^b-human β2m (hβ2m) heterodimers were produced in CHO K1 cells exactly as described in Springer et al. (1998). To remove residual contaminating proteins/peptides from the protein preparation, the purified H-2D^b was denatured and refolded as described in Elliott and Eisen (1990), with the following modifications. Complexes were diluted 1 in 10 in 6 M Guanidine HCl in PBS and dialysed overnight at 4°C. The denatured protein was then concentrated and the heavy and light chains separated by gel

Table 1. Crystallographic Data Collection and Refinement Statistics

Data Collection Statistics

Peptide	Unit Cells (Å)	Resolution (Å)	R_{merge} (%)	Completeness (%)
WT	60.8, 58.1, 74.7	2.85 (2.92–2.85)	9.6 (37.6)	96.1 (86.2)
FAPGNYPAL	$\beta = 108.3$			
K2	60.8, 58.6, 75.3	2.80 (2.88–2.80)	9.5 (42.5)	99.5 (98.4)
FAPGSYPAL	$\beta = 108.5$			
K2G	61.4, 58.4, 77.3	2.60 (2.66–2.60)	5.3 (15.9)	90.2 (61.2)
FAPGS(O-GlcNAc)YPAL	$\beta = 108.9$			
K3G	61.1, 58.3, 77.2	2.65 (2.73–2.65)	6.0 (17.6)	97.0 (95.1)
FAPS(0-GlcNAc)NYPAL	$\beta = 108.6$			

Refinement Statistics

	WT	K2	K2G	K3G
Resolution limits (Å)	10.0-2.85	10.0-2.80	10.0-2.60	10-2.65
n. reflections	11060	11701	14564	14363
n. reflections R_{free} set	1145	1184	1482	1451
R_{free}	28.5	27.3	28.5	26.3
R_{factor}	21.4	21.0	22.7	19.4
n. solvent molecules	26	40	63	105
Rmsd bonds	0.007	0.007	0.008	0.006
Rmsd angles	1.28	1.27	1.34	1.25
Rmsd dihedrals	25.44	25.41	25.67	25.54
Rmsd impropers	1.08	1.05	1.14	1.04
Rmsd for bond B	1.92	1.71	1.71	1.63
Rmsd for angle B	3.28	2.86	2.90	2.76
Average B				
Heavy chain	60	56	57	55
β2-microglobulin	50	48	50	46
Peptide	60	69	76	56

filtration. The H-2D[b] and hβ2m chains were then recombined in 8 M urea and then dialysed against TBS. After further purification by gel filtration, fractions containing the highest amount of B22.249 (Hammerling et al., 1979)-reactive material were pooled and mixed with a 10-fold excess of peptide.

X-Ray Data Collection, Phasing, and Refinement

Crystals were grown by vapor diffusion at 4°C using microbridges (Harlos, 1992) from sitting drops containing 1 ml of protein solution (typically 10 mg/ml H-2D[b] peptide complex in Tris Buffered Saline [pH 7.5]) plus 1 ml of reservoir solution (15%–23% PEG 6000, 100 mM Ammonium Sulphate, and 100 mM MES [pH 5.0]). Crystals were harvested to a modified reservoir solution containing 25% PEG 6000, 100 mM ammonium sulphate, 100 mM sodium chloride, and 50 mM MES [pH 5.0]. For cryo-crystallographic data collection, crystals were transferred stepwise to harvest buffer supplemented with progressively higher concentrations of glycerol up to a final concentration of 20%, flash-cooled in liquid propane, and stored at −170°C in liquid nitrogen. Diffraction data sets were collected at station 7.2 of the Daresbury Synchrotron Light Source, with a MarResearch imaging plate detector, for the WT complex; station BM14 of the European Synchrotron Radiation Facility, using a MarResearch imaging plate for the K3G complex and a CCD detector for the K2G complex; and in house, using a MarResearch imaging plate mounted on a Rigaku RU generator fitted with Yale mirror optics, for the K2 complex. The diffraction data were auto indexed, integrated, scaled, and merged using programs DENZO and SCALEPACK (Otwinowski and Minor, 1997). All crystals belong to the monoclinic space group P2₁ with similar unit cell dimensions. Crystallographic data collection statistics are reported in Table 1. The structure of H-2D[b]/hβ2-m complexed with a mixture of endogenous peptides (data not shown) was solved by molecular replacement with the program AMoRe (Navaza, 1994). The models used were the H-2D[b] heavy chain from the crystal structure of its complex with an influenza virus peptide (Young et al., 1994) (Protein Data Bank identification code 1hoc) and the humanβ2-microglobulin subunit of the HLA-A2 structure (Protein Data Bank identification code 3hla). The rotation and translation searches were carried out independently for three different probes: the H-2D[b] α1/β2 domain (residues 1–174), the H-2D[b] α3

domain (residues 183–272), and the β2-m subunit. Unambiguous solutions were found for the three independent probes that when combined resulted in a correlation coefficient of 0.62 and an R-factor of 0.43, for data between 10.0 and 3.0 Å resolution. The three domains were then rigid-body fitted into the unit cells of the various peptide complexes using X-PLOR (Brunger, 1992). Electron density maps calculated at this stage with coefficients 2Fo-Fc and Fo-Fc showed clear and continuous density in the binding cleft for nine amino acid residues in the WT, K2, and K3G complexes. For the K2G complex, however, weak density was observed between residues P4 to P5, which became better defined at later stages in the structure refinement. Automatic refinement of the four peptide complexes, which included rigid body, overall anisotropic scaling, bulk solvent correction, positional and individual atomic temperature (B), factor refinement, and, occasionally, simulated annealing, was carried out with standard protocols in program X-PLOR and was alternated with manual rebuilding in the interactive graphics program O (Jones, 1985). After extending the resolution to the diffraction limits of each complex, and further refinement until the agreement factor appeared to have reached a minimum (R free between 0.31 to 0.34 and R factor between 0.23 to 0.25, depending on the structure), models of the appropriate peptides were included in the refinements. Since the carbohydrate moieties of the K2G and K3G peptides tended to refine to very high B factors and always showed very weak density in the electron density maps, they were excluded from the models. Density remained clear for the rest of the peptide in the different complexes with the exception of TyrP5 side-chain in the K2 complex structure. For the WT, K2, and K3G complexes, the electron density maps are consistent with a mixture of *cis* and *trans* conformations for the peptide bond N-terminal to the P5-Pro. The mean B value for the protein atoms resulting from the refinements (from 53 Å² to 57 Å²) agree well with those obtained from Wilson plots calculated for the different data sets (ranging from 48 to 61 Å²). For the WT and K3G complexes, the mean B values for the peptide atoms are similar to those for the respective heavy chains. For the low-affinity peptides, K2 and K2G, the mean B values for their peptide atoms are significantly higher that the mean value of the rest of the molecule, perhaps reflecting a partial occupancy.

The statistics of all four refined structures are presented in Table 1.

All have the characteristics of well-refined protein structural models, including good geometry, as defined by PROCHECK (Laskowski et al., 1998), and low values for R free and R factor.

Glycan Mobility Studies by Proton NMR

Samples for NMR were prepared by in vitro refolding of a soluble H2-D^b molecule expressed in *E. coli* around either K2-OGlcNAc or K3G peptide, as described in Rigney et al. (1998). The protein was then exchanged into PBS/D20 using centriprep 10 (Amicon). All spectra were recorded on a Varian Unity 500 spectrometer. Transverse relaxation rates (T2) were measured using a CPMG (Meiboom and Gill, 1958) sequence (90° - {t - 180° - 2t -180° - t}n - aqq) with a 0.00025 sec delay between pulses (t) and the total delay from first pulse t acquisition (4tn) varying from 0.001 to 0.256 sec). X scans were required for adequate signal-to-noise ratios. Spectra were Fourier-transformed directly with no prior mathematical manipulation. The final signal-to-noise ratios obtained were sufficiently high to enable observation of slowly relaxing aromatic side-chains (mainly histidines).

Establishment of CTL Clones and CTL Assays

Peptide- and glycopeptide-specific CTL clones are described in Haurum et al. (1994). The peptide transporter-deficient cell line T2 transfected with H-2D^b (a gift from P. Cresswell, Yale) was used as target cells in conventional chromium release assays for measurement of peptide-specific cytotoxicity mediated by the CTL clones. In some assays, the target cells were prepulsed with an excess of peptide (50 mM) and then labeled with ^{51}Cr (Amersham) before incubation with the CTL clones for 4 hr at 37°C in 96-well plates. In other assays, serial dilutions of peptide (final concentration 50, 5, 0.5, and 0.05 nM) were added directly to the CTL clones and ^{51}Cr labeled target cells.

Molecular Modeling

The framework (V and J segment) sequences for TCR clones K2G.6.9, K3G.5.8, and K3G.6.15 were substituted into the Vα and Vβ domains of a murine TCR crystal structure (Garcia et al., 1996) using MUTATE (Esnouf, 1997). Using program SHP (Stuart et al., 1979), the TCR models for K2G.6.9, K3G.5.8, and K3G.6.15 were positioned onto the TCR in the HLA A2/TCR complex. The correct length CDR3 loops were manually rebuilt in program FRODO (Jones, 1985) using the available murine (Garcia et al., 1996) and human (Garboczi et al., 1996) TCR structures as guides. The crystal structure of the HLA A2/TCR complex of Garboczi and coworkers (Garboczi et al., 1996) was then used as a template to orientate these TCR models relative to the crystal structures of the H-2D^b-K3G and H-2D^b-K2G complexes. The MHC class I structures were positioned by superposition onto HLA A2 using program SHP (Stuart et al., 1979) based on all structurally equivalent Cα atoms of the heavy chain and hβ2m. The resultant series of model complexes were inspected in the interactive graphics program O (Jones et al., 1991).

Acknowledgments

References

Abdel-Motal, U.M., Berg, L., Rosen, A., Bengtsson, M., Thorpe, C.J., Kihlberg, J., Dahmen, J., Magnusson, G., Karlsson, K.A., and Jondal, M. (1996). Immunization with glycosylated Kb-binding peptides generates carbohydrate-specific, unrestricted cytotoxic T cells. Eur. J. Immunol. *26*, 544–551.

Bevan, M.J. (1997). In thymic selection, peptide diversity gives and takes away. Immunity *7*, 175–178.

Brock, R., Weismuller, K., Jung, G., and Walden, P. (1996). Molecular basis for the recognition of two structurally different major histocompatibility complex/peptide complexes by a single T cell receptor. Proc. Natl. Acad. Sci. USA *93*, 13108–13113.

Brünger, A.T. (1992). XPLOR version 3.1: a system for X-ray crystallography and NMR. Department of Molecular Biophysics and Biochemistry, Yale University, New Haven, CT.

Corthay, A., Backlund, J., Broddefalk, J., Michaelsson, E., Goldschmidt, T.J., Kihlberg, J., and Holmdahl, M. (1998). Epitope glycosylation plays a critical role for T cell recognition of type II collagen in collagen-induced arthritis. Eur. J. Immunol. *28*, 2580–2590.

Deck, B., Elofsson, M., Kihlberg, J., and Unanue, E.R. (1995). Specificity of glycopeptide-specific T cells. J. Immunol. *155*, 1074–1078.

Ding, Y.-H., Smith, K.J., Garboczi, D.N., Utz, U., Biddison, W., and Wiley, D.C. (1998). Two human T cell receptors bind in a similar diagonal mode to the HLA-A2/Tax peptide complex using different TCR amino acids. Immunity *8*, 403–412.

Dudler, T., Altmann, F., Carballido, J.M., and Blaser, K. (1995). Carbohydrate-dependent, HLA class II-restricted, human T cell response to the bee venom allergen phospholipase A2 in allergic patients. Eur. J. Immunol. *25*, 538–542.

Elliott, T.J., and Eisen, H.N. (1990). Cytotoxic T lymphocytes recognize a reconstituted class I histocompatibility antigen (HLA-A2) as an allogeneic target molecule. Proc. Natl. Acad. Sci. USA *87*, 5213–5217.

Esnouf, R.M. (1997). An extensively modified version of MolScript that includes greatly enhanced colouring capabilities. J. Mol. Graph. *15*, 133–138.

Fielder, M., Pirt, S.J., Tarpey, I., Wilson, C., Cunningham, P., Ettelaie, C., Binder, A., Bansal, S., and Ebringer, A. (1995). Molecular mimicry and ankylosing spondylitis: possible role of a novel sequence in pullulanase of Klebsiella pneumoniae. FEBS Lett. *369*, 243–248.

Fremont, D.H., Matsumura, M., Stura, E.A., Peterson, P.A., and Wilson, I.A. (1992). Crystal structures of two viral peptides in complex with murine MHC class I H-2Kb. Science *257*, 919–927.

Garboczi, D.N., Madden, D.R., and Wiley, D.C. (1994). Five viral peptide-HLA-A2 co-crystals. Simultaneous space group determination and X-ray data collection. J. Mol. Biol. *239*, 581–587.

Garboczi, D.N., Ghosh, P., Utz, U., Fan, Q.R., Biddison, W.E., and Wiley, D.C. (1996). Structure of the complex between human T-cell receptor, viral peptide and HLA-A2. Nature *384*, 134–141.

Garcia, K.C., Degano, M., Stanfield, R.L., Brunmark, A., Jackson, M.R., Peterson, P.A., Teyton, L., and Wilson, I.A. (1996). An alphabeta T cell receptor structure at 2.5 A and its orientation in the TCR-MHC complex. Science *274*, 209–219.

Garcia, K.C., Degano, M., Pease, L.R., Huang, M.D., Peterson, P.A., Teyton, L., and Wilson, I.A. (1998). Structural basis of plasticity in T cell receptor recognition of a self peptide MHC antigen. Science *279*, 1166–1172.

Hammerling, G.J., Hammerling, U., and Lemke, H. (1979). Immunogenetics *8*, 433–439.

Harding, C.V., Kihlberg, J., Elofsson, M., Magnusson, G., and Unanue, E.R. (1993). Glycopeptides bind MHC molecules and elicit specific T cell responses. J. Immunol. *151*, 2419–2425.

Harlos, K. (1992). Micro-bridges for sitting-drop crystallisations. J. Appl. Crystallog. *25*, 536–538.

Hart, G.W., Haltiwanger, R.S., Holt, G.D., and Kelly, W.G. (1989). Glycosylation in the nucleus and cytoplasm. Annu. Rev. Biochem. *58*, 841–874.

Hart, G.W., Kreppel, L., Comer, F., Arnolds, S., Snow, D., Ye, Z., Cheng, X., Dellamanna, D., Caine, D., Earles, B., et al. (1996). O-GlcNAcylation of key nuclear and cytoskeletal proteins: reciprocity with O-phosphorylation and putative roles in protein multimerisation. Glycobiology *6*, 711–716.

Haurum, J.S. (1996). Recognition of peptides carrying post-translational modifications by class I MHC restricted cytotoxic T cells. D. Phil. Thesis, University of Oxford, Oxford, United Kingdom.

Haurum, J.S., Arsequell, G., Lellouch, A.C., Wong, S.Y., Dwek, R.A., McMichael, A.J., and Elliott, T. (1994). Recognition of carbohydrate by major histocompatibility complex class I-restricted, glycopeptide-specific cytotoxic T lymphocytes. J. Exp. Med. *180*, 739–744.

Haurum, J.S., Tan, L., Arsequell, G., Frodsham, P., Lellouch, A.C., Moss, P.A., Dwek, R.A., McMichael, A.J., and Elliott, T. (1995). Peptide anchor residue glycosylation: effect on class I major histocompatibility complex binding and cytotoxic T lymphocyte recognition. Eur. J. Immunol. *25*, 3270–3276.

Jensen, T., Hansen, P., Galli-Stampino, L., Mouritsen, S., Frische, K., Meinjohanns, E., Meldal, M., and Werdelin, O. (1997). Carbohydrate and peptide specificity of MHC class II-restricted T cell hybridomas raised against an O-glycosylated self peptide. J. Immunol. *158*, 3769–3778.

Jones, T.A. (1985). Diffraction methods for biological macromolecules: interactive computer graphics. FRODO *115*, 157–171.

Jones, T.A., Zhou, J.Y., Cowan, S.W., and Kjelgaard, M. (1991). Improved methods for building protein models in electron density maps and the location of errors in these models. Acta Crystallogr. *A47*, 110–119.

Kast, W.M., Roux, L., Curren, J., Blom, H.J., Voordouw, A.C., Meloen, R.H., Kolakofsky, D., and Melief, C.J. (1991). Protection against lethal Sendai virus infection by in vivo priming of virus-specific cytotoxic T lymphocytes with a free synthetic peptide. Proc. Natl. Acad. Sci. USA *88*, 2283–2287.

Laskowski, R.A., MacArthur, M.W., Moss, D.S., and Thornton, J.M. (1998). PROCHECK. a program to check the stereochemical quality of protein structures. J. Appl. Crystallog. *26*, 283–291.

Madden, D.R. (1998). The three dimensional structure of peptide-MHC complexes. Annu. Rev. Immunol. *13*, 587–622.

Mason, D. (1998). A very high level of crossreactivity is an essential feature of the T cell receptor. Immunol. Today *19*, 395–404.

Meiboom, S., and Gill, D. (1958). Modified spin-echo method for measuring nuclear relaxation times. Rev. Sci. Instruments *29*, 688–691.

Merritt, E.A., and Murphy, M.E.P. (1994). Raster3D version 2.0: a program for photorealistic molecular graphics. Acta Crystallogr. *D50*, 869–873.

Michaelsson, E., Malmstrom, V., Reis, S., Engstrom, A., Burkhardt, H., and Holmdahl, R. (1994). T cell recognition of carbohydrates on type II collagen. J. Exp. Med. *180*, 745–749.

Navaza, Z. (1994). AMoRE—an automated package for molecular replacement. Acta Crystallogr. *A50*, 157–163.

Otwinowski, Z., and Minor, W. (1997). Processing of X-ray diffraction data collected in oscillation mode. Methods Enzymol. *276*, 307–326.

Quiocho, F.A. (1998). Carbohydrate-binding proteins: tertiary structures and protein-sugar interactions. Annu. Rev. Biochem. *55*, 287–315.

Rigney, E., Kojima, M., Glithero, A., and Elliott, T. (1998). A soluble major histocompatibility complex class I peptide-binding platform undergoes a conformational change in response to peptide epitopes. J. Biol Chem. *273*, 14200–14204.

Rotzschke, O., Falk, K., Stevanovic, S., Jung, G., Walden, P., and Rammensee, H.G. (1991). Exact prediction of a natural T cell epitope. Eur. J. Immunol. *21*, 2891–2894.

Sinha, A., Lopez, T., and McDevitt, H.O. (1990). Autoimmune disease: the failure of self tolerance. Science *248*, 1380–1388.

Smith, K.J., Reid, S.W., Stuart, D.I., McMichael, A., Bell, J.I., and Jones, E.Y. (1996). Bound water structure and polymorphic amino acids act together to allow the binding of different peptides to MHC class I HLA-B53. Immunity *4*, 215–228.

Springer, S., Doring, K., Skipper, J., Townsend, A., and Cerundolo, V. (1998). Fast association rates suggest a conformational change in the MHC class I molecule H-2D^b upon peptide binding. Biochemistry *37*, 3001–3021.

Steinman, L. (1996). Multiple sclerosis: a co-ordinated immunological attack against myelin in the central nervous system. Cell *85*, 299–302.

Stuart, D.I., Levine, M., Muirhead, H., and Stammers, D.K. (1979). The crystal structure of cat pyruvate kinase at a resolution of 2.6A. J. Mol. Biol. *134*, 109–142.

Teng, M.-K., Smolyar, A., Tse, A.G.D., Liu, J.-H., Liu, J., Hussey, R.E., Nathenson, S.G., Chang, H.-C., Reinherz, E.L., and Wang, J.-H. (1998). Identification of a common docking topology with substantial variation among different TCR-peptide-MHC complexes. Curr. Biol. *8*, 409–412.

van Eden, W., Thole, J., van der Zee, R., Noordzij, A., van Embden, J., Hensen, E., and Cohen, I.R. (1988). Cloning of the mycobacterial epitope recognised by T lymphocytes in adjuvant arthritis. Nature *331*, 171–173.

Wormald, M.R., Rudd, P.M., Harvey, D.J., Chang, S.C., Scragg, I.G., and Dwek, R.A. (1997). Variations in oligosaccharide-protein interactions in immunoglobulin G determine the site-specific glycosylation profiles and modulate the dynamic motion of the Fc oligosaccharides. Biochemistry *36*, 1370–1380.

Wucherpfennig, K., and Strominger, J.L. (1995). Molecular mimicry in T cell mediated autoimmunity: viral peptides activate human T cell clones specific for myelin basic protein. Cell *80*, 695–705.

Young, A.C., Zhang, W., Sacchettini, J.C., and Nathenson, S.G. (1994). The three-dimensional structure of H2-Db at 2.4A resolution: implications for antigen determinant selection. Cell *76*, 39–50.

Zhao, X.J., and Cheung, N.K. (1995). GD2 oligosaccharide: target for cytotoxic T lymphocytes. J. Exp. Med. *182*, 67–74.

Brookhaven Protein Data Bank ID Codes

Atomic coordinates for the H-2D^b-K3G and H-2D^b-K2G complexes have been deposited with the Protein Data Bank, Brookhaven National Laboratory, and are available prerelease from yvon@biop. ox.ac.uk.